Magnetic Flux Density of a Circular Loop Derived from the Vector Potential: A New Approach

Bendaoud Saâd

Cadi Ayyad University, National School of Applied Sciences of Safi, MISCOM Laboratory, Morocco

Abstract: Circular current loops are foundational to understanding electromagnetic devices like solenoids and transformers, with critical applications in metal detection, magnetic confinement, and wireless power transfer. Although the magnetic flux density field along the loop's axis is easily derived, calculating it at arbitrary off-axis points is analytically challenging, often leading to treatments that present results without a clear derivation. This study addresses this gap by providing a detailed, pedagogical calculation of the magnetic flux density, B, derived rigorously from the magnetic vector potential, A. While calculations are possible in Cartesian or spherical coordinate systems, we demonstrate that the cylindrical coordinate system is preferable, as it naturally exploits the cylindrical symmetry of the problem. This choice leads to a logically streamlined path to the solution, which is elegantly formulated in terms of complete elliptic integrals of the first and second kind. The derivation yields explicit expressions for the radial and axial field components at any point in space, while the azimuthal component vanishes due to symmetry. As a critical validation, we recover the standard elementary expression for in-plane and on-axis fields as a limiting case of the general solution. This work consolidates classical results into a unified and transparent framework that serves a dual purpose: it demystifies the underlying mathematics for students and educators. It provides a reliable, efficient analytical tool for benchmarking numerical simulations in engineering and research. By clarifying the derivation from first principles, this study strengthens the theoretical foundation for modeling circular current loops and broadens their practical applicability.

Keywords: Circular current loop . Magnetic flux density . Biot-Savart law . Vectro Potential . Elliptic integrals .

1. Introduction

The magnetic flux density field generated by a circular current loop is a foundational problem in electromagnetism, with critical applications spanning physics and engineering, from the design of solenoids and transformers to particle accelerators and magnetic resonance imaging. While the field along the loop’s axis is readily derived from the Biot-Savart law and is a staple of undergraduate curricula [1-4], the determination of the field at arbitrary off-axis points presents a significant challenge. Direct application of the Biot-Savart law for any point yields integrals that resist expression in elementary functions, necessitating the use of special functions such as complete elliptic integrals.

This challenge is not merely academic. Cylindrical coils with helical windings, such as solenoids, are fundamentally modeled as superposition of individual circular loops. Consequently, an accurate and general analytical expression for the field of a single loop is essential for modeling these complex systems [5–6]. Two primary analytical approaches exist for this problem: the direct integration of the Biot-Savart law and the computation of the magnetic flux density (**B**) as the curl of the magnetic vector potential (**A**). The relative simplicity of each method depends on the specific geometry and the desired outcome, yet a clear, pedagogical comparison focusing on the vector potential approach is often lacking in the literature.

Indeed, while the analytical expressions for the off-axis field components are well-known and have been presented in various forms, their detailed derivations are frequently omitted. For instance, the axial and radial components of **B** are often stated without demonstration [7–9], as exact calculations are straightforward only along the loop's axis. This has led to a situation where undergraduate students typically only compute the axial field, while the more complex off-axis problem is avoided. Historical and contemporary works, from Smythe's

1989 classical treatment [10] and Callaghan and Maslen's analysis of finite solenoids [11] to more recent publications by Simpson et al. [8] and González and Cárdenas [12-13], provide the results but often in a form that is dense and difficult for students and practitioners to follow. Smythe's treatment, while comprehensive, is particularly concise, underscoring the need for a more transparent and pedagogical derivation.

Therefore, although circular current loops are widely studied, a comprehensive and accessible treatment of the magnetic flux density at any point in space, derived rigorously from the vector potential, remains limited. This study aims to fill this gap by providing a systematic and pedagogically clear derivation of the magnetic field generated by a filamentary, planar, circular current loop. The primary objective is to elucidate the path from the vector potential **A** to the flux density **B** (**B**=∇×**A**) in cylindrical coordinates, leveraging the inherent symmetry of the problem.

The specific objectives of this work are:

1. To present a step-by-step derivation of the magnetic vector potential and its subsequent curl, expressing the components of **B** explicitly in terms of complete elliptic integrals of the first and second kinds.
2. To demonstrate the recovery of the elementary on-axis field expression as a limiting case of the general solution, thereby validating the derived expressions.
3. To provide a unified framework that is both rigorous and accessible, serving as a valuable resource for education and as a reliable benchmark for numerical simulations in research and engineering applications.

By offering a transparent and detailed calculation, this study not only clarifies the underlying mathematics but also provides a robust analytical tool for accurately modeling magnetic fields in applications ranging from sensor design to the analysis of complex electromagnetic systems.

2. Materials, Methods, and the Vector Potential Calculation

2.1. Problem Geometry and Symmetry Analysis

We consider a filamentary, planar, circular loop of radius R carrying a steady current I. The loop lies in the z = 0 plane, centered on the origin of a cylindrical coordinate system (ρ, φ, z), as depicted in **Fig. 1**.

In cylindrical coordinates, the general expression of the vector potential at any point P in space should be written as follows:

$$\mathbf{A} = A_\rho(\rho,\varphi,z)\,\boldsymbol{u}_\rho + A_\varphi(\rho,\varphi,z)\,\boldsymbol{u}_\varphi + A_z(\rho,\varphi,z)\boldsymbol{u}_z \tag{1}$$

The inherent symmetries of the system dictate the form of the magnetic vector potential, **A**. The circular loop is invariant under rotations around the z axis. Furthermore, any plane containing the z axis (a ρ-z plane) is an antisymmetry plane for the current distribution. Because **A** is a **true vector**, it must be perpendicular to these antisymmetry planes. This symmetry analysis leads to two critical conclusions:

1. The components of **A** contained within the ρ-z plane must be zero (A_ρ = 0 and A_z = 0) and the Eq. (1) of the vector potential simplifies to:

$$\mathbf{A}(\rho,\varphi,z) = A_\varphi(\rho,\varphi,z)\,\boldsymbol{u}_\varphi \tag{2}$$

2. The only non-vanishing component is azimuthal, A_φ, and due to rotational symmetry, it cannot depend on the azimuthal angle φ. Therefore, the vector potential simplifies to:

$$\mathbf{A}(\rho, z) = A_{\varphi}(\rho, z)\,\boldsymbol{u}_{\varphi} \tag{3}$$

where A_{φ} is a function only of ρ and z. This establishes the implicit form of the potential before its explicit calculation.

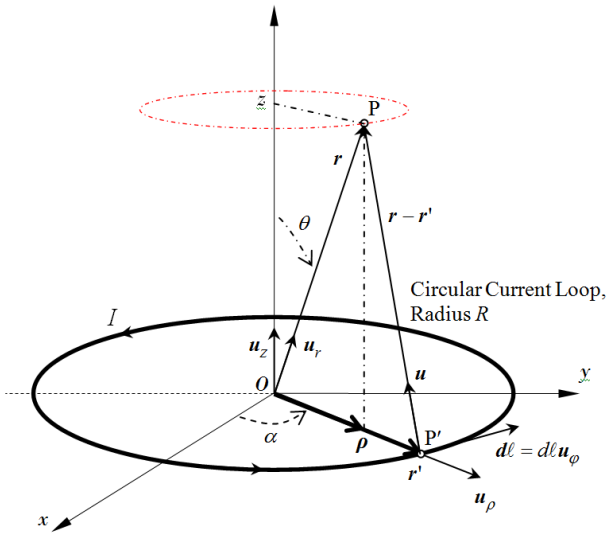

Figure 1. Current loop lies in *x*-*y* plane. The field point P has cylindrical coordinate (ρ, z).

2.2. Magnetic Vector Potential Determination

For a filamentary loop C, the magnetic vector potential at a field point $\boldsymbol{r}$ is given by [14,15]:

$$\mathbf{A}(r) = \frac{\mu_0}{4\pi} \oint_C \frac{I d\ell}{\|\boldsymbol{r} - \boldsymbol{r}'\|} \tag{4}$$

where $\boldsymbol{d}\ell$ is the differential length segment of the loop at the source point P′ indicated by the position vector $\boldsymbol{r}'$, and μ_0 is the permeability of free space.

The position vector $\boldsymbol{r}$, indicating point P, can be written as:

$$\begin{aligned} \boldsymbol{r} &= r\boldsymbol{u}_r \\ &= \rho\,\boldsymbol{u}_{\rho} + z\,\boldsymbol{u}_z \end{aligned} \tag{5}$$

where $\rho = r\sin\theta$, and $z = r\cos\theta$ (6)

Exploiting the rotational symmetry, we perform the calculation in the *x*-*z* plane without loss of generality. In this plane, the field point is $\boldsymbol{r} = (\rho, 0, z)$. A source point on the loop can be parameterized by the angle α as:

$$\boldsymbol{r}' = (R\cos\alpha, R\sin\alpha, 0) \tag{7}$$

The displacement vector from the source point P′ to the observation point P is:

$$\boldsymbol{r} - \boldsymbol{r}' = (\rho - R\cos\alpha, -R\sin\alpha, z) \tag{8}$$

Subsequently, the distance between the source and field points is:

$$\|\boldsymbol{r}-\boldsymbol{r}'\| = \sqrt{R^2+\rho^2+z^2-2R\rho\cos\alpha)} \tag{9}$$

The corresponding differential length element is:

$$\boldsymbol{d\ell} = Rd\alpha\,\boldsymbol{u}_\varphi = R\,d\alpha(-\sin\alpha\,\boldsymbol{i}+\cos\alpha\,\boldsymbol{j}) \tag{10}$$

Substituting relations (10) and (11) into the integral for **A** [Eq. (4)], the general expression for φ=0 is:

$$\mathbf{A}(\rho,z) = A_\varphi(\rho,z)\,\boldsymbol{u}_\varphi = \frac{\mu_0 I}{4\pi} R \int_0^{2\pi} \frac{-\sin\alpha\,d\alpha\,\boldsymbol{i}+\cos\alpha\,d\alpha\,\boldsymbol{j}}{(R^2+\rho^2+z^2-2R\rho\cos\alpha)^{1/2}} \tag{11}$$

The ***i***-component integrates to zero over $\alpha\in[0,2\pi]$ due to symmetry.

To demonstrate this, assume that

$$f(\alpha) = (R^2+\rho^2+z^2-2R\rho\cos\alpha)^{1/2} \quad \Rightarrow \quad \frac{df}{d\alpha} = \frac{R\rho\sin(\alpha)}{(R^2+\rho^2+z^2-2R\rho\cos\alpha)^{1/2}}, \text{ then}$$

$$\mathbf{A}(\rho,z)\boldsymbol{i} = A_\varphi(\rho,z)\,\boldsymbol{u}_\varphi.\boldsymbol{i} = -\frac{\mu_0 I}{4\pi}\int_0^{2\pi} \frac{R\sin\alpha\,d\alpha}{(R^2+\rho^2+z^2-2R\rho\cos\alpha)^{1/2}}$$

$$= -\frac{\mu_0 I}{4\pi}\frac{1}{\rho}\int_0^{2\pi} \frac{\rho R\sin\alpha}{(R^2+\rho^2+z^2-2R\rho\cos\alpha)^{1/2}}d\alpha$$

$$= -\frac{\mu_0 I}{4\pi}\frac{1}{\rho}\int_0^{2\pi} \frac{df}{d\alpha}d\alpha$$

$$= -\frac{\mu_0 I}{4\pi}\frac{1}{\rho}\left[(R^2+\rho^2+z^2-2R\rho\cos\alpha)^{1/2}\right]_0^{2\pi}$$

$$= -\frac{\mu_0 I}{4\pi}\frac{z}{\rho}\left[(R^2+\rho^2+z^2-2R\rho)^{1/2}-(R^2+\rho^2+z^2-2R\rho)^{1/2}\right]$$

$$= 0$$

We find the vector potential has only a ***j***-component in the *x*-*z* plane. Thus, Eq. (11) simplifies to:

$$\mathbf{A}(\rho,z) = A_\varphi(\rho,z)\,\boldsymbol{u}_\varphi = \frac{\mu_0 I}{4\pi}\int_0^{2\pi} \frac{R\cos\alpha\,d\alpha}{(R^2+\rho^2+z^2-2R\rho\cos\alpha)^{1/2}}\boldsymbol{j} \tag{12}$$

Since $\boldsymbol{j}$ corresponds to $\boldsymbol{u}_\varphi$ at $\varphi=0$, the general expression for any φ is:

$$\mathbf{A}(\rho,z) = \frac{\mu_0 I}{4\pi}\int_0^{2\pi} \frac{R\cos\alpha\,d\alpha}{(R^2+\rho^2+z^2-2R\rho\cos\alpha)^{1/2}}\boldsymbol{u}_\varphi \tag{13}$$

This is the fundamental analytical expression for the vector potential of circular current loops. At the center of the loop, $A_\varphi(0,0)=0$, and at the loop's filament, $A_\varphi(R,0)=10\,\mu_0 I/(4\pi R)$.

2.3. Formulation in Terms of Complete Elliptic Integrals

The integral for A_φ is evaluated by expressing it in terms of standard complete elliptic integrals. Exploiting the evenness of the integrand, the limits can be reduced to [0,π]:

$$A_\varphi(\rho,z)=\frac{\mu_0 I}{2\pi}R\int_0^{\pi}\frac{\cos\alpha\,d\alpha}{(R^2+\rho^2+z^2-2R\rho\cos\alpha)^{1/2}} \tag{14}$$

At this stage, integration by substitution is employed by introducing the following change of variable:

$$\alpha=\pi-2\beta,\ d\alpha=-2d\beta\ .\ \text{If}\ \ \alpha=0\ \text{then}\ \beta=\frac{\pi}{2}\ ,\ \text{and if}\ \alpha=\pi\ \ \text{then}\ \beta=0$$

$$\cos(\alpha)=\cos(\pi-2\beta)=\cos(2\beta-\pi)=-\cos(2\beta)=2\sin^2(\beta)-1 \tag{15}$$

Following the substitution, Eq. (14) becomes:

$$A_\varphi(\rho,z)=\frac{\mu_0 I}{\pi}R\int_0^{\pi/2}\frac{2sin^2\beta-1}{\sqrt{R^2+\rho^2+z^2+2R\rho-4R\rho\,sin^2\beta}}d\beta \tag{16}$$

Let us pose $\mu=k^2=\dfrac{4\rho R}{q}$ where $q=R^2+\rho^2+z^2+2\rho R=(R+\rho)^2+z^2$ (17)

where k is the modulus of Jacobian elliptic functions [15-16].

By substituting relations (17) into (16), ultimately we get:

$$A_\varphi(\rho,z)=\frac{\mu_0 I}{\pi}\frac{R}{\sqrt{q}}\int_0^{\pi/2}\frac{2sin^2\beta-1}{\sqrt{1-k^2\,sin^2\beta}}d\beta \tag{18}$$

After algebraic manipulation, the integral for $A_\varphi(\rho,\varphi)$ becomes a linear combination of two standard complete elliptic integrals. Thus, Eq. (18) can be rewritten in the following form:

$$A_\varphi(\rho,z)=\frac{\mu_0 I}{\pi}\frac{R}{\sqrt{q}}\left\{\frac{2}{k^2}\left[\int_0^{\pi/2}\frac{d\beta}{\sqrt{1-k^2\,sin^2\beta}}-\int_0^{\pi/2}\sqrt{1-k^2\,sin^2\beta}\,d\beta\right]-\int_0^{\pi/2}\frac{d\beta}{\sqrt{1-k^2\,sin^2\beta}}\right\} \tag{19}$$

Among these two integrals, one can be identified as the complete elliptic integral of the first kind, commonly denoted $K(k)$, which is defined as [17-18]:

$$K(k)=\int_0^{\pi/2}\frac{d\beta}{\sqrt{1-k^2sin^2\beta}} \tag{20}$$

Especially, at $k=0$, $K(0)=\pi/2$; when $k\to 1$, $K(k)\to\infty$.

According to Arfken & Weber [17] and Weisstein [19], when $k^2=1$, the function value is infinite.

For $0 \le k^2 < 1$, the function value is finite but increases as k^2 increases, as shown in **Fig. 2**.

The other integral in Eq. (20) can be identified as the complete elliptic integral of the second kind, commonly denoted $E(k)$, which is defined as [16, 19-20]:

$$E(k) = \int_0^{\pi/2} \sqrt{1 - k^2 \sin^2 \beta}\, d\beta \tag{21}$$

For $k^2 = 0$, $E(0) = \pi/2$, for $k^2 = 1$, then $E(1) = 1$.

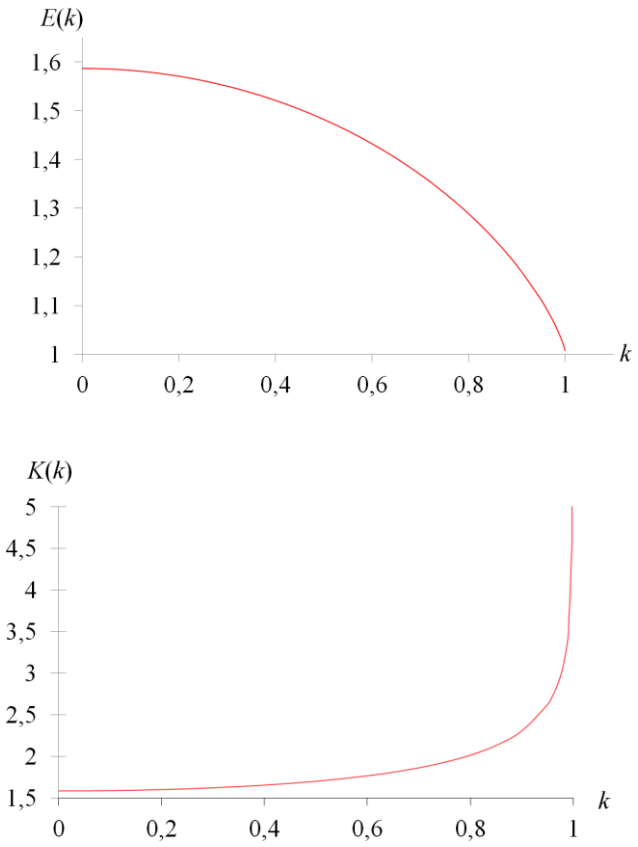

Figure 2. Complete elliptic integral of the first and second kind as a function of the modulus k.
At $k^2 = 1$, $K(k)$ diverges, *i.e.*, when $k^2 \to 1$, $K(k) \to \infty$.

Reexamining Eq. (19), it is evident that it encompasses the special case of the complete elliptic integral of the first and second kinds. Accordingly, the vector potential can be expressed as:

$$A_\varphi(\rho, z) = \frac{\mu_0 I}{\pi} \frac{R}{\sqrt{q}} \left\{ \frac{2}{k^2} (K(k) - E(k)) - K(k) \right\} \tag{22}$$

which leads to the following standard form after rearranging [10-11]:

$$A_\varphi(\rho, z) = \frac{\mu_0 I}{\pi} \sqrt{\frac{R}{\rho}} \frac{1}{k} \left[\left(1 - \frac{1}{2} k^2 \right) K(k) - E(k) \right] \tag{23}$$

Rearranging, Eq. (23) becomes [21]:

$$A_\varphi(\rho,z)=\frac{\mu_0}{4\pi}\frac{4IR}{\sqrt{(R+\rho)^2+z^2}}\left[\frac{(2-k^2)K(k)-2E(k)}{k^2}\right] \tag{23}$$

This is a **canonical form** of the vector potential of current loops. This expression for A_φ (ρ, z) is valid for all points in space except the line ρ = 0 (on-axis), where the limit must be taken separately. En effect, at ρ = 0 the factor $\sqrt{R/\rho}$ is singular but the bracket tends to zero in such a way that the limit is zero.

2.4. In-Plane and On-Axis Potential Calculation

The magnetic vector potential A_φ for any point in space can be computed by determining the parameter k from Eq. (17) and using tabulated values of the complete elliptic integrals $K(k)$ and $E(k)$. This provides an analytical approach via Eq. (23). An alternative is the direct numerical evaluation of the integral form given by Eq. (13). This section details the numerical methodology and presents the results for the specific case of points lying within the plane of the loop itself.

Owing to the loop's axisymmetric geometry, the vector potential is purely azimuthal. As established by Eqs. (3) and (13), the field points strictly perpendicular to the ρ-z plane. Consequently, by symmetry, the bi-dimensional distribution is fully characterized by calculating the potential along a single radial line in the plane, with the complete field distribution obtained by azimuthal rotation.

To simplify the numerical calculation, we introduce normalized spatial variables:

$$a=\frac{\rho}{R}\ ,\quad b=\frac{z}{R} \tag{24}$$

where R is the loop radius. This transformation renders Eq. (13) into a dimensionless form:

$$A_\varphi(\rho,z)=\frac{\mu_0 I}{4\pi}\frac{1}{R}\int_0^{2\pi}\frac{\cos\alpha}{(1+a^2+b^2-2a\cos\alpha)^{1/2}}d\alpha \tag{25a}$$

In-Plane condition, *i.e.*, z=0 (θ=π/2 in **Fig. 1**), b=0 and a=r/R, where r is the radial coordinate. Under this condition, Eq. (25a) simplifies to a form suitable for numerical integration. The integral was evaluated using a discretization approach. The numerical approximation of the integral is given by:

$$A_\varphi(a)\approx\sum_{i=1}^{N}F(a,\alpha_i)\Delta\alpha \tag{25b}$$

where $F(a,\alpha_i)=\frac{\mu_0}{4\pi}\frac{I}{R}\frac{cos(\alpha_i)}{(1+a^2-2a\,cos(\alpha_i))^{1/2}}$, $\alpha_i=\frac{\alpha_{n+1}+\alpha_n}{2}$ are the discrete angular values,

and $\Delta\alpha=2\pi/N$ is the constant step size. The accuracy of this approximation increases with the number of steps N. For this study, a value of N=200 was selected, providing a robust compromise between computational efficiency and precision ($a_0= 0$, $a_1= 2\pi/200$, $a_2= a_1+2\pi/200$, $a_3= a_2+2\pi/200$, …, $a_{200}= a_{199}+2\pi/200= 2\pi$).

The normalized vector potential A_φ computed using this numerical method is presented in **Table 1** as a function of the relative radius $a=r/R$. The corresponding curve is also visualized in **Fig. 3**. The curve shows that the integral in Eq. (25a) is therefore continuous, vanishing at the center of the loop and asymptotically approaching zero with $a \to \infty$. In contrast, its value on the loop's filament is finite.

Table 1. Normalized Magnetic Vector Potential in the Plane of the Circular Loop.

$a = r/R$	$A_\varphi/\mu_0 I/(4\pi R)$	$a = r/R$	$A_\varphi/\mu_0 I/(4\pi R)$
0,00	0,00	1	9,99
0,10	0,32	1,02	7,79
0,20	0,64	1,04	6,48
0,30	0,98	1,06	5,67
0,40	1,34	1,08	5,09
0,50	1,75	1,1	4,64
0,60	2,22	1,12	4,28
0,70	2,80	1,14	3,98
0,8	3,59	1,16	3,72
0,82	3,80	1,18	3,49
0,84	4,02	1,2	3,29
0,86	4,28	1,3	2,55
0,88	4,58	1,4	2,07
0,9	4,92	1,5	1,73
0,92	5,35	1,6	1,47
0,94	5,90	1,7	1,27
0,96	6,66	1,8	1,11
0,98	7,91	1,9	0,98
1	9,99	2	0,87

Positive sign of the potential indicates that the vector A_φ is oriented in the direction of the unit vector $\boldsymbol{u}_\varphi$ implied by the current direction, consistent with the right-hand rule.

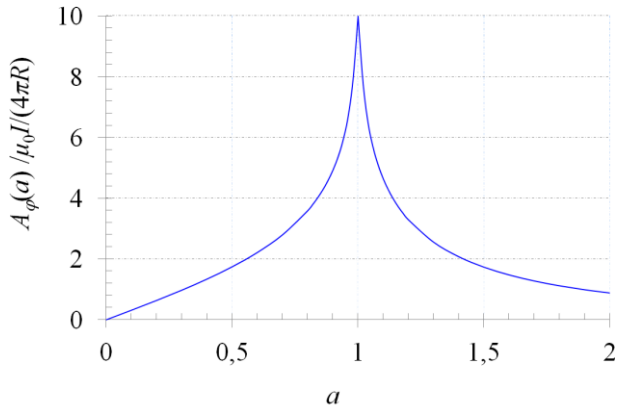

Figure 3. Magnetic vector potential amplitude in the plane of a circular loop as a function of the normalized radius. The potential vanishes at the center (a=0) and has a finite limit at a=1.

To accurately model a physical conductor with finite volume and avoid the unphysical singularities associated with idealized line currents, the vector potential must be formulated in terms of a more general

volume integral. Within the conductor's cross-section, the potential is thus finite and governed by an expression of the form [21, 22]:

$$\mathbf{A}(\boldsymbol{r}) = \frac{\mu_0}{4\pi} \oint_c \frac{\mathbf{J}(\boldsymbol{r}')}{\|\boldsymbol{r} - \boldsymbol{r}'\|} d^3 r' \tag{26}$$

where **J** is the current density and μ_0 is the permeability of vacuum.

Furthermore, for comparison, the analytical expression of Eq. (23) was also evaluated for the in-plane case. With $k^2=4a/(1+a)^2$, it reduces to

$$A_\varphi(a) = \frac{\mu_0 I}{\pi} \frac{(1+a)}{2a} \left[\frac{1+a^2}{(1+a)^2} K(k) - E(k) \right] \tag{27}$$

The results from this analytical method are in exact agreement with the numerical integration, producing the same curve shown in **Fig. 3**. This validates the numerical procedure.

Finally, it is noted that on the axis of the loop ($\rho=0$,$a=0$), the parameter $k^2=0$. Since $K(0)=E(0)=\pi/2$, Eq. (23) confirms that the vector potential is zero at all points on the z axis, as required by symmetry.

3. Magnetic Flux Density Derivation from the Vector Potential

In cylindrical coordinates, the implicit function of the magnetic flux density vector in 3D-space is:

$$\mathbf{B}(\rho, \varphi, z) = B_\rho(\rho, \varphi, z)\, \boldsymbol{u}_\rho + B_\varphi(\rho, \varphi, z)\, \boldsymbol{u}_\varphi + B_z(\rho, \varphi, z)\, \boldsymbol{u}_z \tag{28}$$

The inherent symmetries of the system dictate the form of the magnetic flux density vector, **B**. The circular loop is invariant under rotations around the z axis. Furthermore, any plane containing the z axis (a ρz-plane) is an antisymmetry plane for the current loop. Because **B** is a **pseudovector**, it must be contained in these antisymmetry planes. This symmetry analysis leads to two critical conclusions:

3. The components of the flux density vector **B** contained within the ρ-z plane must be non-zero ($B_\rho \neq 0$ and $B_z \neq 0$), the azimuthal component vaniches by symmetry ($B_\varphi=0$) and Eq. (28) reduces to

$$\mathbf{B}(\rho, \varphi, z) = B_\rho(\rho, \varphi, z)\, \boldsymbol{u}_\rho + B_z(\rho, \varphi, z)\, \boldsymbol{u}_z \tag{29}$$

4. The field possesses no azimuthal component. Therefore, the general expression for the flux density vector simplifies to

$$\mathbf{B}(\rho, z) = B_\rho(\rho, z)\, \boldsymbol{u}_\rho + B_z(\rho, z)\, \boldsymbol{u}_z \tag{30}$$

This establishes the implicit form of the flux density before its explicit calculation.

The magnetic flux density **B** is related to the vector potential via the curl operation, **B**=∇×**A**, a relation that holds under the Coulomb gauge (∇·**A**=0). In cylindrical coordinates, the curl of **A** [Eq. (1)] is given by:

$$\mathbf{B}=\nabla\times\mathbf{A}=\left(\frac{1}{\rho}\frac{\partial A_z}{\partial\varphi}-\frac{\partial A_\varphi}{\partial z}\right)\boldsymbol{u}_\rho+\left(\frac{\partial A_\rho}{\partial z}-\frac{1}{\rho}\frac{\partial A_z}{\partial\rho}\right)\boldsymbol{u}_\varphi+\frac{1}{\rho}\left(\frac{\partial(\rho A_\varphi)}{\partial\rho}-\frac{\partial A_\rho}{\partial\varphi}\right) \tag{31}$$

From symmetry, the vector potential possesses only an azimuthal component, A_φ, which is a function solely of ρ and z, *i.e.*, A_ρ=0 and A_z=0. Applying these conditions to Eq. (31) yields the components of **B**:

$$B_\rho=-\frac{\partial A_\varphi}{\partial z},\quad B_\varphi=0,\quad B_z=\frac{1}{\rho}\frac{\partial(\rho A_\varphi)}{\partial\rho} \tag{32}$$

This result is consistent with the form postulated in Eq. (30).

The subsequent derivations detail the calculation of these components from this formulation.

The following derivatives are needed to continue [15-17]:

$$\frac{dK(k)}{dk}=\frac{E(k)}{k(1-k^2)}-\frac{K(k)}{k} \tag{33}$$

$$\frac{dE(k)}{dk}=\frac{E(k)-K(k)}{k} \tag{34}$$

3.1. Radial component $B_\rho(\rho, z)$

From Eq. (32), the radial component is given by $B_\rho=-\partial A_\varphi/\partial z$. To compute this derivative, we use Eq. (23) which expresses A_φ as a function of the modulus k, which itself is a function of ρ and z.

Applying the chain rule:

$$\frac{\partial A_\varphi}{\partial z}=\frac{dA_\varphi}{dk}\frac{\partial k}{\partial z} \tag{35}$$

From (17), we have:

$$\frac{\partial k}{\partial z}=-\frac{4R\rho z}{k((R+\rho)^2+z^2)^2}=-\frac{zk^3}{4\rho R} \tag{36}$$

Express A_φ given by the function (23) as a function of k.

Let

$$f(k)=(1-\frac{1}{2}k^2)K(k)-E(k) \tag{37}$$

so that

$$A_{\varphi}(\rho,z)=\frac{\mu_0 I}{\pi}\sqrt{\frac{R}{\rho}}\frac{f(k)}{k} \tag{38}$$

Dufferentiating A_{φ} with respect to k:

$$\frac{dA_{\varphi}(\rho,z)}{dk}=\frac{\mu_0 I}{\pi}\sqrt{\frac{R}{\rho}}\frac{d}{dk}\left(\frac{f(k)}{k}\right)=\frac{\mu_0 I}{\pi}\sqrt{\frac{R}{\rho}}.\frac{k\,f'(k)-f(k)}{k^2} \tag{39}$$

Differentiating $f(k)$ with respect to k,

$$f'(k)=-kK(k)+(1-\frac{1}{2}k^2)K'(k)-E'(k) \tag{40}$$

By substituting $K'(k)$ and $E'(k)$ by (33) and (34) respectively,

$$f'(k)=-kK(k)+(1-\frac{1}{2}k^2)\frac{E(k)-(1-k^2)K(k)}{k(1-k^2)}-\frac{E(k)-K(k)}{k} \tag{41}$$

Simplifying,

$$f'(k)=k\left(-\frac{1}{2}K(k)+\frac{1}{2(1-k^2)}E(k)\right) \tag{42}$$

Substituting in Eq. (39) and doing algebraic operations, Eq. (39) becomes:

$$\frac{dA_{\varphi}(\rho,z)}{dk}=\frac{\mu_0 I}{\pi}\sqrt{\frac{R}{\rho}}\left(-\frac{K(k)}{k^2}+\frac{2-k^2}{2k^2(1-k^2)}E(k)\right) \tag{43}$$

Substituting Eqs. (36) and (43) into Eq. (35), we obtain:

$$\frac{\partial A_{\varphi}(\rho,z)}{\partial z}=\frac{\mu_0 I}{\pi}\sqrt{\frac{R}{\rho}}\left(\frac{K(k)}{k^2}-\frac{2-k^2}{2k^2(1-k^2)}E(k)\right).\frac{zk^3}{4\rho R} \tag{44}$$

The two minus signs cancel.

Simplifying by using again $k^2=\frac{4R\rho}{q}=\frac{4R\rho}{(R+\rho)^2+z^2}$ given by Eq. (17) and rearranging terms yields:

$$\frac{\partial A_{\varphi}(\rho,z)}{\partial z}=-\frac{\mu_0 I}{\pi}\sqrt{\frac{R}{\rho}}\frac{1}{(R+\rho)^2+z^2}\frac{z}{k}\left(-K(k)+\frac{2-k^2}{2(1-k^2)}E(k)\right) \tag{45}$$

A significant simplification is achieved by substituting the geometric relation $\frac{1}{k}\sqrt{\frac{R}{\rho}} = \frac{\sqrt{(R+\rho)^2+z^2}}{2\rho}$, then Eq. (45) becomes:

$$\frac{\partial A_\varphi(\rho,z)}{\partial z} = -\frac{\mu_0 I}{2\pi}\frac{1}{\sqrt{(R+\rho)^2+z^2}}\frac{z}{\rho}\left(-K(k)+\frac{2-k^2}{2(1-k^2)}E(k)\right) \tag{46}$$

Substituting k^2 by its expression in Eq. (17) again and after algebraic manipulations, the elliptic fraction equals the geometric ratio as follows:

$$\frac{2-k^2}{2(1-k^2)} = \frac{2-\frac{4R\rho}{R^2+\rho^2+z^2+2R\rho}}{2(1-\frac{4R\rho}{R^2+\rho^2+z^2+2R\rho})} = \frac{R^2+\rho^2+z^2}{(R-\rho)^2+z^2}$$

Substituting, Eq. (46) yields

$$\frac{\partial A_\varphi(\rho,z)}{\partial z} = -\frac{\mu_0 I}{2\pi}\frac{1}{\sqrt{(R+\rho)^2+z^2}}\frac{z}{\rho}\left(-K(k)+\frac{R^2+\rho^2+z^2}{(R-\rho)^2+z^2}E(k)\right) \tag{47}$$

From Eq. (32), the **canonical form** of $B_\rho(\rho,z)$ finally is:

$$B_\rho(\rho,z) = \frac{\mu_0}{2\pi}\frac{I}{\sqrt{(R+\rho)^2+z^2}}\frac{z}{\rho}\left(-K(k)+\frac{R^2+\rho^2+z^2}{(R-\rho)^2+z^2}E(k)\right) \tag{48}$$

3.2. Axial component $B_z(\rho,z)$

From Eq. (32), the axial component is given by:

$$B_z = \frac{1}{\rho}\frac{\partial(\rho A_\varphi)}{\partial\rho} \tag{49}$$

So first compute $\rho A_\varphi(\rho,z)$, for this, multipling Eq. (23) by ρ as follows:

$$\rho A_\varphi(\rho,z) = \frac{\mu_0 I}{\pi}\rho\sqrt{\frac{R}{\rho}}\frac{1}{k}\left[\left(1-\frac{1}{2}k^2\right)K(k)-E(k)\right] \tag{50}$$

Simplifing by the square root factor:

$$\rho A_\varphi(q,k) = \frac{\mu_0 I}{\pi}\sqrt{\rho R}\frac{1}{k}\left[\left(1-\frac{1}{2}k^2\right)K(k)-E(k)\right] \tag{51}$$

Differentiate Eq. (49) with respect to ρ as follows:

$$B_z(\rho,z)=\frac{1}{\rho}\frac{\partial}{\partial\rho}(\rho A_\varphi)$$
$$=\frac{\mu_0 I}{\pi}\frac{1}{\rho}\frac{\partial}{\partial\rho}\left(\frac{\sqrt{\rho R}}{k}\left[\left(1-\frac{1}{2}k^2\right)K(k)-E(k)\right]\right) \quad (52)$$

This derivative involves three types of dependences:

1. Explicit $\sqrt{\rho}$ dependence forme the $\sqrt{\rho R}$.
2. $k(\rho)$ dependence in the denominator and inside the bracket.

   Recall from Eq. (17) that: $k^2=\frac{4R\rho}{(R+\rho)^2+z^2}$.

   So both numerator and denominator depend on ρ.
3. Dependence of $K(k)$ and $E(k)$ on k. For this, we need derivatives given by Eqs. (33) and (34) above.

   So the derivative is a product and chain rule problem.

Let's define for clarty:

$$f(k)=(1-\frac{1}{2}k^2)K(k)-E(k),\quad g(\rho,k)=\frac{\sqrt{\rho R}}{k}\Rightarrow \rho A_\varphi(\rho,z)=\frac{\mu_0 I}{\pi}g(\rho,k)f(k) \quad (53)$$

Substituting $f(k)$ [**Eq. (37)**] and $g(\rho, k)$ into Eq. (52), we obtain:

$$B_z(\rho,z)=\frac{\mu_0 I}{\pi}\frac{1}{\rho}\frac{\partial}{\partial\rho}\left(g(\rho,k).f(k)\right)$$
$$=\frac{\mu_0 I}{\pi}\frac{1}{\rho}\left(g'(\rho,k).f(k)+g(\rho,k).f'(k)\right) \quad (54)$$

where $g'(\rho,k)=\frac{\partial g(\rho,k)}{\partial\rho}$ and $f'(k)=\frac{df(k)}{dk}\frac{\partial k}{\partial\rho}$.

Below, we compute $\frac{\partial k}{\partial\rho}$, $\frac{df(k)}{dk}$ and $\frac{\partial g(\rho,k)}{\partial\rho}$, then combine and simplify.

From (17), we obtain:

$$\frac{\partial k}{\partial\rho}=\frac{dk}{dk^2}\frac{\partial k^2}{\partial\rho}=\frac{1}{2k}\frac{\partial k^2}{\partial\rho}=\frac{2R(R^2-\rho^2+z^2)}{k((R+\rho)^2+z^2)^2} \quad (55)$$

and from Eq. (42),

$$\frac{df(k)}{dk}=\frac{k}{2(1-k^2)}(E(k)-(1-k^2)K(k)) \quad (56)$$

Differentiate $g(\rho,k)$ with respect to ρ and using product + chain rule:

$$g'(\rho,k)=\frac{\partial g(\rho,k)}{\partial\rho}=\frac{1}{2k}\sqrt{\frac{R}{\rho}}-\frac{\sqrt{R\rho}}{k^2}\frac{\partial k}{\partial\rho} \quad (57)$$

Combine (55), (56) and (57), and after all algebra (lots of cancellations with the chain rule), Eq. (57) condenses beautifully into the known compact formula:

$$B_z(\rho,z)=\frac{\mu_0 I}{2\pi}\frac{1}{\sqrt{(R+\rho)^2+z^2}}\left(K(k)+\frac{R^2-\rho^2-z^2}{(R-\rho)^2+z^2}E(k)\right) \tag{58}$$

Equations (48) and (58) provide the **canonical formulas** for the magnetic flux density field of a circular current loop in a closed analytical form involving complete elliptic integrals of the first and second kinds.

4. Results

Consequently, we arrive at explicit expressions for the magnetic flux density field vector components in (30) as in (32). The azimuthal component is zero, $B_\varphi(\rho,z)=0$. The radial and axial components of the magnetic flux density field vector of a circular current loop at every point in space are as follows:

$$B_\rho(\rho,z)=\frac{\mu_0}{2\pi}\frac{I}{\sqrt{(R+\rho)^2+z^2}}\frac{z}{\rho}\left(-K(k)+\frac{R^2+\rho^2+z^2}{(R-\rho)^2+z^2}E(k)\right) \tag{48}$$

$$B_z(\rho,z)=\frac{\mu_0 I}{2\pi}\frac{1}{\sqrt{(R+\rho)^2+z^2}}\left(K(k)+\frac{R^2-\rho^2-z^2}{(R-\rho)^2+z^2}E(k)\right) \tag{58}$$

The calculations of the complete elliptic integrals into Eqs. (20) and (21) can be performed using software such as MATLAB, MATHEMATİCA, and ALGLIB Elliptic Integral subroutines for C++ / Java / Python.

Numerical values of B_ρ and B_z can be computed for any values of ρ and z by finding k from (23) and looking up the corresponding values of $K(k)$ and $E(k)$ in the corresponding tables.

5. Analysis of the Magnetic Flux Density

With the vector potential established and the general expressions for the magnetic flux density components B_ρ and B_z derived, we now analyze the field in two critical configurations: within the plane of the loop and along its central axis. These cases provide valuable insight into the field's behaviour and allow for direct comparison with well-known results.

5.1. Field Distribution in the Plane of the Loop

The magnetic flux density field within the plane of the loop (z=0 plane) exhibits a high degree of symmetry [23]. The radial component B_ρ vanishes everywhere in this plane, resulting in a field that is strictly perpendicular to it. It is therefore sufficient to compute the field along a single radial axis, with the full two-dimensional distribution obtained by rotational invariance.

To facilitate this analysis, we use the normalized coordinates $a=\rho/R$ and $b=z/R$ [Eq. (24)], where ρ and z are already in Eq. (6). Eqs. (48) and (58) become:

$$B_\rho(\rho,z)=\frac{\mu_0 I}{2\pi}\frac{b}{\sqrt{q}}\left(-K(k)+\frac{1+a^2+b^2}{(1-a)^2+b^2}E(k)\right) \tag{59}$$

$$B_z(\rho,z)=\frac{\mu_0 I}{2\pi}\frac{1}{\sqrt{q}}\left(K(k)+\frac{1-a^2-b^2}{(1-a)^2+b^2}E(k)\right) \tag{60}$$

Substituting $b=0$ into Eqs. (59) and (60), and noting again that for $z=0$, $a=r/R$, we find that the radial component $B\rho$ is identically zero. The axial component, however, is non-zero and simplifies to:

$$B_z(a)=\frac{\mu_0 I}{2\pi R}\frac{1}{(1+a)}\left(K(k)+\frac{1+a}{1-a}E(k)\right) \tag{61}$$

where $k^2=4a/(1+a)^2$.

At the very center of the loop ($a=0$), the parameter $k^2=0$, and the complete elliptic integrals take the values $K(0)=E(0)=\pi/2$. Equation (61) thus reduces to the classic result:

$$B_z(0)=\frac{\mu_0 I}{2R} \tag{62}$$

Normalizing the general expression (61) by the central field (62) yields the dimensionless field strength in the plane of the loop:

$$\frac{B_z(a)}{B_z(0)}=\frac{1}{\pi}\frac{1}{(1+a)}\left(K(k)+\frac{1+a}{1-a}E(k)\right) \tag{63}$$

The evaluation of Eq. (63) relies on the computation of the complete elliptic integrals, a task for which modern mathematical software (e.g., MATLAB, Python's SciPy) provides robust numerical routines. Care must be taken in the numerical evaluation as $a\to1$, where $k^2\to1$, as this is a singular limit for these integrals.

The profile of the normalized flux density, given by Eq. (63) and plotted in **Fig. 4**, reveals several key features. The field is finite and maximal at the center ($a=0$) and is continuous for both $a<1$ (inside the loop) and $a>1$ (outside the loop), asymptotically vanishing as $a\to\infty$. A divergence appears precisely at $a=1$, which corresponds to the location of the current filament itself. This unphysical singularity is a direct consequence of modeling the loop as a one-dimensional, zero-thickness conductor. In any physical circuit with finite cross-sectional dimensions, the field at the conductor's edge remains finite [22].

The sign of B_z is positive for $a<1$ and negative for $a>1$. This reflects the direction of the magnetic field lines: inside the loop, the field is oriented along the positive z axis, while outside, it points in the negative z-direction as shown in **Fig. 5**, forming closed loops that circulate around the current-carrying wire.

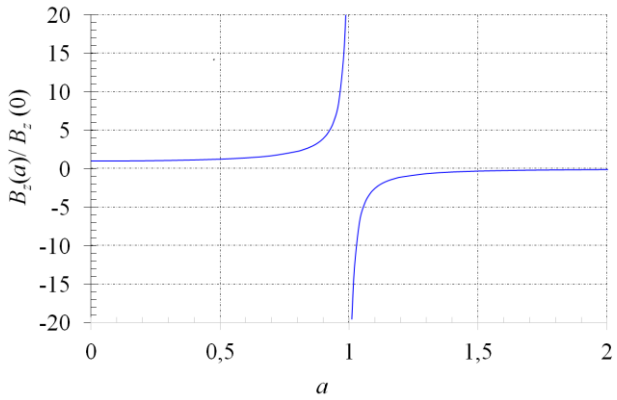

Figure 4. Normalized magnetic flux density $B_z/B_z(0)$ in the plane of a circular current loop as a function of the normalized radial distance $a=r/R$. The divergence at $a=1$ is an artifact of the idealized filamentary current model.

5.2. Field Distribution Along the Axis of the Loop

The field along the loop's axis ($\rho=0$) represents another case where the general expressions simplify considerably. Substituting $a=0$ and $b=z/R$ into Eqs. (59) and (60), we find $k^2=0$, $K(0)=E(0)=\pi/2$, and the radial component B_ρ vanishes identically. The axial component reduces to the well-known expression:

$$B_z(0,z)=\frac{\mu_0 I}{2}\frac{R^2}{(R^2+z^2)^{3/2}} \tag{64}$$

This is the classic result for the on-axis field of a circular loop which found in the most textbooks of Magnetostatics. The field is purely axial, as required by symmetry, and decreases with distance $|z|$ from the loop's center [24-27]. By using Eq. (24), we obtain:

$$B_z(0,z)=\frac{\mu_0 I}{2R}\frac{1}{(1+b^2)^{3/2}} \tag{65}$$

where $b = z/R$.

6. Conclusion

This article has presented a rigorous and pedagogically clear derivation of the magnetic flux density, **B**, for a circular current loop by starting from the magnetic vector potential, **A**. We have demonstrated that the use of a cylindrical coordinate system is not merely convenient but logically imperative, as it naturally exploits the system's symmetry and provides the most streamlined mathematical pathway.

The central result of this work is a set of exact, general expressions for the magnetic induction components, elegantly formulated in terms of complete elliptic integrals of the first and second kinds. This approach successfully unifies the treatment of both on-axis and off-axis fields, demonstrating that the well-known elementary formula is a specific limiting case of this comprehensive solution. Beyond its pedagogical value in

demystifying a classic problem, this formulation serves as a vital analytical tool. It provides a precise, closed-form benchmark for validating numerical simulations in computational electromagnetics, which is critical for the design of devices like solenoids and wireless power transfer systems [28-30].

By clarifying the direct path from the vector potential to the physically measurable magnetic induction field, this work strengthens the theoretical foundation for modeling circular currents. The methodology established here is readily extendable to more complex systems, such as multi-loop solenoids, ensuring its continued relevance in both academic and engineering contexts.

Acknowledgments

We acknowledge the generous support provided by Cadi Ayyad University for this work.

Conflict of Interest

The author declares that he has no conflicts of interest.

References

[1] Ida, N. (2015) Engineering Electromagnetics. 3rd Edition. Springer, 390–391.

[2] Plonus, M. A. (1978) Applied Electromagnetics. McGraw-Hill Inc., New York, 221–222.

[3] Serway, R. A., Jewett, J. W. (2014) Physics for Scientists and Engineers with Modern Physics. 9th Edition. Brooks/Cole CengageLearning, Boston (2014), 908–909.

[4] Young, H. D., Freedman, R. A., Ford, A. L.: Sears and Zemansky's University Physics: with modern physics. 13th Edition, Addison-Wesley Pearson Education Inc. (2012), 932–934.

[5] Jang, T., Ha, H. J., Seo, Y. K., Sohn, S. H.: Off-axis magnetic fields of a circular loop and a solenoid for the electromagnetic induction of a magnetic pendulum. J. Phys. Commun. **5**(**6**):065003 (2021).

[6] Jang T, Seo, Y. K., Sohn, S. H., Jung, J.: Calculation of the off-axis Magnetic Field for Finite-length Solenoids. New Phys.: Sae. Mulli. **70**, 667–674 (2020).

[7] Breneman, B. C., Purcell, J. R., Burnett, S. C.: Magnetic resonance imaging system and method of manufacturing thereof. European Patent number EP 0 310 212 A2, GA Technologies Inc. (1989).

[8] Simpson, J. C., Lane, J. E., Immer, C. D., Youngquist, R. C.: Simple Analytic Expressions for the Magnetic Field of a Circular Current Loop. The NASA Technical Reports Server, 1–7 (2001). Retrieved March 8, 2025, from https://ntrs.nasa.gov/citations/20010038494.

[9] Trebbin, G.: Off-axis Magnetic Field of a Circular Current Loop, (2012). https://www.grant-trebbin.com/2012/04/off-axis-magnetic-field-of-circular.html Retrieved February 18, 2025, from https://youtu.be/SJtbeg_PZ30.

[10] Smythe, W. R.: Static and Dynamic Electricity. Taylor & Francis Inc. (1989), 290–291.

[11] Callaghan, E. E., Maslen, S. H.: The magnetic field of a finite solenoid. NASA Technical note, 1–23 (1960). https://ntrs.nasa.gov/citations/19980227402

[12] González, M., Cárdenas, D.: Analytical Expressions for the Magnetic Field Generated by a Circular Arc Filament Carrying a Direct Current. IEEE Access, **9**, 7483–7495 (2021).

[13] Schill, R. A.: General relation for the vector magnetic field of a circular current loop: a closer look. IEEE Trans. Magn., **39**(2), 961–967 (2003).

[14] Boridy, E.: Électromagnétisme : théorie et applications. 5th Ed., Presses de l'Université de Québec, Canada (1990), 421–422.

[15] Good, R. H.: Elliptic integrals, the forgotten functions. Eur. J. Phys. **22**(2), 119–126 (2001).

[16] Saâd, B.: Electric Field Derivation from the Scalar Potential of a Filamentary Plane Uniformly Charged Ring at Any Point in Space. European Eur. J. Electr. Eng. Comput. Sci. **9** (5), 22-30.

[17] Arfken, G. B., Weber, H. J.: Mathematical Methods for Physicists. Elsevier Academic Press, New York (2005), 372–376.

[18] Noh, H. R. Electrostatic potential of a charged ring: Applications to elliptic integral identities. J. Korean Phys. Soc. **71**, 37–41 (2017). https://doi.org/10.3938/jkps.71.37

[19] Weisstein, E. W.: Elliptic Integrals. Wolfram Research Inc https://mathworld.wolfram.com/

[20] Gradshteyn, I. S., Ryzhik, I. M.: Table of integrals, series, and products. (Scripta Technica, Inc., Trans.). Elsevier Inc. (A. Jeffrey, Ed.; D. Zwillinger, Ed.; V. Moll, Sci. Ed.), (2007).

[21] Jackson, J. D.: Classical Electrodynamics. 3rd Ed., John Wiley & Sons, Inc., New York . London . Sydney 1999, pp. 181–184.

[22] William H. Hayt, W. H., Buck, J. A.: Engineering Electromagnetics. Mc Graw Hill (2012), 222.

[23] Trebbin, G.: Off-axis Magnetic Field of a Circular Current Loop, (2015). https://www.grant-trebbin.com/2015/12/in-plane-magnetic-field-of-current-loop.html

[24] Karimian, S. and Mehrshahi, G.: Accurate off-axis magnetic field calculation of axisymmetric cylindrical current distributions. AIP Advances **11**:095107, 1–9 (2021).

[25] Behtouei, M., Faillace, L., Spataro, B., Variola, A., Migliorati, M.: A novel exact analytical expression for the magnetic field of a solenoid. Waves Random Complex Media **32**(4), 1977–1991 (2020). doi: https://doi.org/10.1080/17455030.2020.1842554

[26] Behtouei, M.; Bacci, A.; Carillo, M.; Comelli, M.; Faillace, L.; Migliorati, M.; Verra, L.; Spataro, B.: Numerical and Analytical Study of the Magnetic Field Distribution in a Three-Solenoid System. *Fractal* **9**:383 (2025). https://doi.org/10.3390/ fractalfract9060383

[27] Behtouei, M.; Bacci, A.; Carillo, M.; Comelli, M.; Faillace, L.; Migliorati, M.; Verra, L.; Spataro, B.: Numerical and Analytical Study of the Magnetic Field Distribution in a Three-Solenoid System. *Fractal* **9**:383 (2025). https://doi.org/10.3390/ fractalfract9060383

[28] Luo, W.-J., Dwi Kuncoro, C. B., Sunkar, P., and Kuan, Y.-D.: Single-Layer Transmitter Array Coil Pattern Evaluation toward a Uniform Vertical Magnetic Field Distribution. Energies **12**(21):4157 (2019). doi : 10.3390/en12214157.

[29] Ortner, M.; Leitner, P.; Slanovc, F.: Numerically Stable and Computationally Efficient Expression for the Magnetic Field of a Current Loop. *Magnetism* **3**, 11–31 (2023).

[30] Chapman, G. H., Carleton, D. E., and Sahota, D. G. Current Loop Off Axis Field Approximations With Excellent Accuracy and Low Computational Cost. *IEEE Transactions on Magnetics* **58**(8):1–6 (2022). doi : 10.1109/TMAG.2022.3149010.